WIND TUNNEL VALIDATION OF A PARTICLE TRACKING MODEL TO ASSESS THE WIND-INDUCED UNDERCATCH OF RAINFALL GAUGES

Arianna Cauteruccio [1,2], Mattia Stagnaro [1,2], Elia Brambilla [3], Luca G. Lanza [1,2*] & Daniele Rocchi [3]

(1) Department of Civil, Chemical and Environmental Engineering, University of Genova, Genoa, Italy
(2) WMO/CIMO Lead Centre "B. Castelli" on Precipitation Intensity, Italy
(3) Department of Mechanical Engineering, Politecnico di Milano, Milan, Italy

**email: luca.lanza@unige.it*

KEY POINTS

- *Particle-fluid interactions as induced by the outer geometry of catching type gauges are studied*
- *A Lagrangian Particle Tracking model for liquid particles is implemented*
- *A dedicated setup is used for the wind tunnel validation of the simulated trajectories*

1 INTRODUCTION

The external design of catching type precipitation gauges has a major impact on the catch efficiency in windy conditions due to the bluff-body aerodynamics of their outer geometry. This topic can be investigated by using CFD simulations of the airflow field surrounding the gauge body and by adopting a Lagrangian Particle Tracking (LPT) model to evaluate the influence of the airflow deformation on the trajectory of the approaching hydrometeors.

The earliest study on the modelling of hydrometeors trajectories was published by *Mueller & Kidder* (1972); in that work, particle trajectories were simulated based on the flow field measured in the wind tunnel using hot film anemometers. *Folland* (1988) later developed two simplified trajectory models based on the flow velocity and direction obtained in the vertical plane centred on the gauge collector along the main flow direction partially published by *Robinson & Rodda* (1969) and described by *Warnik* (1953). The trajectory models were based on the equation of motion of the particles. In the first model a 2-D numerical solution was obtained and then extended to a 3-D model considering the variation of the orifice width in the transversal direction. The second model uses geometrical considerations to calculate the number of particles falling outside instead of inside of the gauge collector. In the work of *Nešpor & Sevruk* (1999), the airflow velocity field around three cylindrical gauges was calculated by numerically solving the Reynolds Average Navier-Stokes equations based on a turbulence closure model and liquid particle trajectories were modelled. This simulation scheme was adopted also by *Thériault et al.* (2012) and *Colli et al*. (2015) for solid precipitation, by increasing the details of the computational mesh to better capture the airflow features. In the work of *Thériault et al.* (2012) a fixed drag coefficient for each crystal type was adopted while *Colli et al.* (2015) obtained a better comparison with real-world data by calculating the snowflake trajectories while accounting for the dependence of the aerodynamic drag coefficient on the local Reynolds number of solid particles.

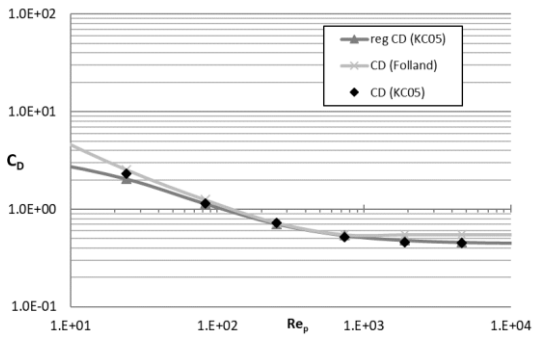

Figure 1. Comparison between the raw data proposed by KC05, the best-fit curve and the formulation proposed by *Folland* (1988).

In the present work a literature LPT model, improved by *Colli et al.* (2015) and applied to solid precipitation, was adapted to simulate the trajectories of water droplets when falling through the atmosphere

and approaching the gauge collector by introducing suitable drag coefficient equations. The innovative contribution of this work is the validation of the LPT model by means of wind tunnel tests conducted by realizing a dedicated setup able to release water drops in the WT and to detect their deviation when approach the gauge and travel above the collector. Very few literature works, *Warnik* (1953) and *Green & Helliwell* (1972), report same attempts to detect water drops in the wind tunnel. In the present work, water droplets are generated and tracked at high resolution in the WT, using a high speed camera.

2 METHODOLOGY

2.1 Lagrangian Particle Tracking model

The LPT model, based on the equation of particle motion, allows to follow the trajectory of a single particle immersed in a fluid by describing its properties at each time interval. The trajectories are computed with a forward step procedure by calculating at short time intervals the particle positions. The particle tracking model is run upon the disturbed airflow field calculated by means of Computation Fluid Dynamics simulations for the desired gauge geometry and wind speed. In the present work, the improved LPT model used by *Colli et al.* (2015) was adopted. In the model the drag coefficient of a falling particle is influenced by the instantaneous particle-to-air magnitude of velocity through the particle Reynolds number (Re_p) and at each time step the particle trajectory is obtained by updating the Reynolds number and the associated Drag Coefficient (C_D).

In the present work liquid particles were parameterized with a spherical shape of equivalent diameter *d*. The particle density was set equal to 1000 kg m^{-3} at the air temperature of 20°C. The C_D values as a function of Re_p proposed by *Khvorostyanov and Curry* (2005), hereafter KC05, for spherical particles in turbulent condition, were fitted with a three parameters inverse proportionality function. The relations proposed by *Folland* (1988) were also compared with the raw data provided by KC05 as shown in **Figure *1***. Based on this comparison the best-fit curve obtained from KC05 was implemented in the particle tracking model for Re_p values larger than 400, while the equations proposed by Folland were adopted for Re_p lower than 400.

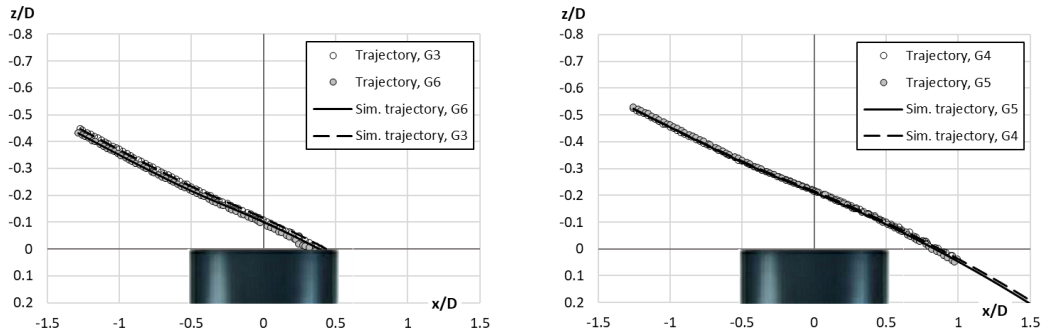

Figure 2. Observed (circles) and simulated (lines) drop trajectories above the collector of a chimney shaped gauge (U_{ref} = 10.2 ms^{-1}).

2.2 Validation setup

Wind tunnel tests were carried out on a chimney-shaped gauge, the GeonorT200B®, in the wind tunnel facility available at Politecnico di Milano within the activities of the PRIN 20154WX5NA project. The wind tunnel was equipped with a hydraulic system to generate droplets, a high-speed camera and a high-power lamp to shot and illuminate droplets along their trajectories. The hydraulic system consists of a water tank which feeds a volumetric pump (model Ismatec Reglo-Z digital) connected to a nozzle. The tests were conducted using a fixed flow rate of 0.8 ml/min and a nozzle orifice size of 0.008''. The support for the nozzle was shaped to have a reduced impact on the airflow close to the orifice and to minimize the oscillations at the edge where droplets are released. To capture the drop trajectories, the high-speed camera was placed in front of the gauge and the recording speed was set to 1000 fps, with an image resolution of 1600x900 pixels, the dimension of the image was 40 x 20 cm with the pixel size of 0.2370 mm. The tests were conducted in a dark environment while backlighting the gauge from above using an incandescent lamp. The investigated precipitation gauge was positioned downstream of the drop generator, so that drops are released along the symmetry axis of the gauge parallel to the wind direction. The path of each drop is

identified by many frames: in every frame the drop is in a given position, which evolves in the next frame. Due to the reduced exposure time of each image, few light hits the camera sensor and the image appears dark. To increase the visibility of the drops, each image was then converted to greyscale and a combination of a Gaussian and Laplacian filter was applied. The image was binarized using a threshold level, with the zeroes indicating the background while the ones indicate the presence of the drop. Finally, using a moving window over the image, the center of the drop was identified and stored. Finally, knowing the time interval between two subsequent images and the conversion rate from pixels to mm, it was also possible to calculate the drop speed in the 2-D shooting plane.

3 RESULTS

The validation of the Particles Tracking model was obtained by comparison between observed and simulated trajectories. In the numerical model the initial conditions, position and velocity, of the simulated trajectories were set consistently with the wind tunnel observations. The initial velocity components were set equal to the mean values of the three to five initial positions of each drop as shot by the camera, so as to avoid the noise due to the uncertainty in the initial positions. **Figure *2*** and **Figure *3*** show the comparison between observed and simulated drop trajectories, above the collector of a chimney shaped gauge at a wind speed U_{ref} = 10.2 ms^{-1}. The initial conditions of each drop, used to run the numerical model, are listed in **Table *1***. Each observed drop trajectory is characterized by the undisturbed part, unaffected by the aerodynamic response of the gauge, which was linearity interpolated and by the disturbed part that was fitted with a third order polynomial. The slope curve of each observed trajectory was obtained as the first derivative of the fitted trajectories. In left-hand panel of **Figure *2*** the initial elevation (z/D) of the two droplets is not much different. As expected, the derived slope curves have revealed that the trajectory which travels closer to the gauge body is deviated earlier from its undisturbed condition. The undisturbed slopes, which are characterized by a constant value and depend on the wind speed and the drops size but are independent from the aerodynamic response of the gauge, revealed that the two droplets have the same size. This assumption is confirmed by the numerical trajectories because the optimal agreement between the observed and simulated trajectories is reached by setting the drop diameter equal to one millimetre for both trajectories. The observed and simulated trajectories are not totally overlapped close to the downwind edge of the collector. This effect is probably ascribable to the installation of the gauge in the wind tunnel, where a slight inclination was observed due to the push load induced by the wind on the gauge body. The good repeatability of the trajectories of very similar drops in the wind tunnel is shown in the right-hand panel of **Figure *2***. By injecting drops of the same size in the wind tunnel the observed trajectories are indeed very close to each other, and they experience the same deviation above the collector. The LPT model is able to replicate even the small variations due to slight differences in the initial conditions about the drop velocity.

ID	Wind [ms^{-1}]	x/D	z/D	u [ms^{-1}]	w [ms^{-1}]	d [mm]
G3	10.2	-1.272	-0.447	3.968	-1.151	1
G6	10.2	-1.284	-0.433	3.809	-1.095	1
G2	10.2	-1.259	-0.690	4.286	4.286	1.2
G4	10.2	-1.257	-0.523	4.140	1.104	1
G5	10.2	-1.257	-0.523	4.122	1.122	1

Table 1. Wind tunnel flow velocity, initial coordinates and velocity components for the simulated drop trajectories and the resulting drop diameter.

According to the PIV airflow velocity fields reported by *Stagnaro et al.* (2020), the calculated horizontal acceleration of the drop, depicted in the left-hand panel of Figure 3, normalized with the one experienced in the initial undisturbed part of the trajectory, shows that the drop significantly accelerates when travelling above the upwind part of the collector until crossing the separation layer between the airflow recirculation and accelerated zones, when it starts decelerating abruptly towards the downwind edge of the collector. This drop is released at a higher elevation than the previous drops; the observed and simulated trajectories show a good overlap also in the second half part of the trajectory, where the aerodynamic effect of the gauge is less sensible to the non-perfect orthogonality of the installation. The maximum difference between observed and simulated trajectories (red markers) arises in the upwind edge of the collector and is about 1.2 mm. This

difference is fully comparable to the drop size (see Table 1), therefore is comparable with the uncertainty in the assessment of the drop position, identified as a bright moving object in each frame.

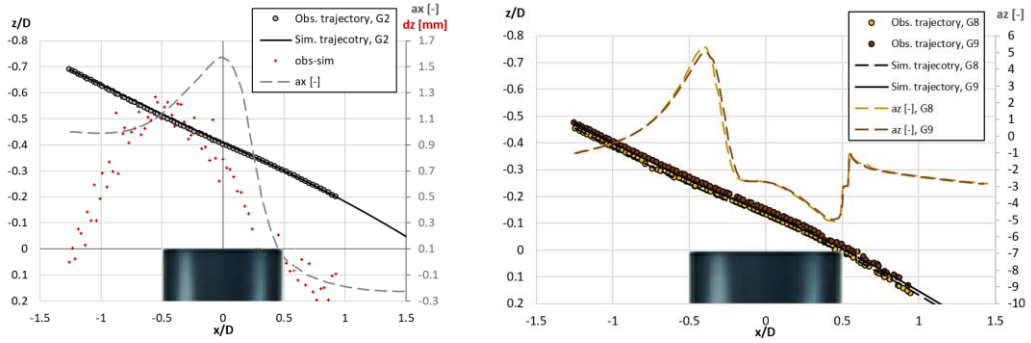

Figure 3. Observed (circles) and simulated (continuous line) drop trajectories above the collector of a chimney shaped gauge at a wind speed U_{ref} = 10.2 ms^{-1}. In the left-hand panel the difference between the vertical positions of the observed and simulated drop trajectories (red markers) is reported in the right-hand axis together with the normalized numerical longitudinal acceleration of the drop (dashed line). In the right-hand panel the trajectories and their normalized numerical vertical accelerations are depicted.

Finally, a comparison of two simulated trajectories is shown in the right-hand panel of Figure 3, together with the observed ones. Also in this case, the difference between observed and simulated trajectories is comparable with the uncertainty in the assessment of the drop position. Dashed lines represent the normalized numerical vertical acceleration of the drop along the trajectories calculated by the LPT model. The two drops accelerate when reaching the upwind edge due to the updraft and then decelerate due to the downdraft; this behaviour is in line with the measured PIV velocity field (*Stagnaro et al.* 2020).

4 CONCLUSIONS

The deviated trajectories of the drops detected in the wind tunnel allowed to clearly visualise the wind-induced undercatch of catching-type precipitation gauges. The observed trajectories closely reproduce the modelled ones therefore validating the numerical model and confirming that the formulation used for the drag coefficient is suitable to reproduce the observed behaviour of the hydrometeors when affected by the airflow deformation due to the bluff-body aerodynamics of precipitation gauges. The numerical model can be applied to calculate the Collection Efficiency curves which allow to correct the wind-induced error on precipitation measurements by varying the gauge geometry, wind speed and type of precipitation.

Acknowledgements
This work was developed in the framework of the Italian national project PRIN20154WX5NA "Reconciling precipitation with runoff: the role of understated measurement biases in the modelling of hydrological processes".

REFERENCES

Colli, M., Lanza, L.G., Rasmussen, R., Thériault, J.M., Baker, B.C. & Kochendorfer, J. An improved trajectory model to evaluate the collection performance of snow gauges. Journal of Applied Meteorology and Climatology, 2015, 54, 1826–1836.

Folland, C.K. Numerical models of the raingauge exposure problem, field experiments and an improved collector design. Quarterly Journal of the Royal Meteorological Society, 1988, 114, 1485–1516.

Green, M.J. & Helliwell, P. R. The effect of wind on the rainfall catch. Distribution of precipitation in mountainous areas. World Meteorological Organization, 1972, Rep. 326, Vol. 2, 27–46.

Khvorostyanov, V.I., & Curry, J.A. Fall Velocities of Hydrometeors in the Atmosphere: Refinements to a Continuous Analytical Power Law. Journal of the Atmospheric Sciences, 2005, 62, 4343–4357.

Mueller C.C. & Kidder, E.H. Rain gage catch variation due to airflow disturbances around a standard rain gage. Water Resources Research, 1972, 8(4), 1077-1082.

Nešpor, V. & Sevruk, B. Estimation of wind-induced error of rainfall gauge measurements using a numerical simulation. Journal of Atmospheric and Oceanic Technology, 1999, 16, 450 - 464.

Robinson, A.C. & Rodda, J.C. Rain wind and aerodynamic characteristics of rain-gauges. Meteorol. Mag., 1969, 98, 113-120.

Stagnaro, M., Cauteruccio, A., Brambilla, E., Lanza, L.G. & Rocchi, D. Wind tunnel tests to evaluate the rain drops deviations around different type of precipitation gauges. XXXVII Conv. Naz. Idraulica e Costruzioni Idrauliche, Reggio Calabria, 2020.

Warnik, C.C. Experiments with windshields for precipitation gages. Trans. American Geophysical Union, 1953, 34(3), 379 – 388.